JPET #172395

Silencing MAP Kinase-activated Protein Kinase-2 Arrests Inflammatory Bone Loss

Qiyan Li, Hong Yu, Robert Zinna, Kylie Martin, Bethany Herbert, Angen Liu, Carlos Rossa, Jr., and Keith L. Kirkwood

Department of Craniofacial Biology, Medical University of South Carolina, Charleston, SC (Q. L., H. Y., B. H., C. R. Jr., K. L. K.), Center for Oral Health Research, Medical University of South Carolina, Charleston, SC (Q. L., H. Y., R. Z., K. M., C. R. Jr., K. L. K.), Department of Biology, College of Charleston, Charleston, SC (B. H.), Hollings Cancer Center Biorepository, Medical University of South Carolina, Charleston, SC (A. L.), Department of Microbiology and Immunology, Medical University of South Carolina, Charleston, SC (K.L.K.)

1

Running Title: MK2 siRNA attenuates periodontal disease progression

Correspondence:

Keith L. Kirkwood, DDS, PhD

Department of Craniofacial Biology, College of Dental Medicine, Medical University of South

Carolina, 173 Ashley Ave., Charleston, SC 29425

Tel: (843) 792-0969, Fax: (843) 792-5312, E-mail: klkirk@musc.edu

Number of text Pages: 30

Number of Tables: 0

Number of Figures: 6

Number of References: 28

Number of words in Abstract: 178

Number of words in Introduction: 585

Number of words in Discussion: 845

Abbreviations: MAPKs, mitogen-activated protein kinases; MK2, mitogen-activated protein kinase-activated protein kinase 2; siRNA, small interfering RNA; NF-κB, nuclear factor-kappa B; TNF-α, tumor necrosis factor-alpha; MMPs, matrix metalloproteinases; μCT, microcomputed tomography; BVF, bone volume fraction; LCM, laser capture microdissection; TRAP, tartrate resistant acid phosphatase; H&E, hematoxylin and eosin; ROI, region of interest

Recommended section assignment: Inflammation, Immunopharmacology, and Asthma

ABSTRACT

p38 mitogen-activated protein kinases (MAPKs) are critical for innate immune signaling and subsequent cytokine expression in periodontal inflammation and bone destruction. In fact, previous studies show that systemic p38 MAPK inhibitors block periodontal disease progression. However, development of p38 MAPK inhibitors with favorable toxicological profiles is difficult. Here we report our findings regarding the contribution of the downstream p38 MAPK substrate, mitogen-activated protein kinase-activated protein kinase 2 (MAPKAPK-2 or MK2), in immune response modulation in an experimental model of pathogen-derived lipopolysaccharide (LPS)-induced periodontal bone loss. To determine whether small interfering RNA (siRNA) technology had intraoral applications, we initially validated MK2 siRNA MK-2 specificity. Then, gingival tissue surrounding maxillary molars of rats was injected with MK2 siRNA or scrambled siRNA at the palatal regions of bone loss. Intraoral tissues treated with MK2 siRNA had significantly less MK2 mRNA expression compared with scrambled siRNA-treated tissues. MK2 siRNA delivery arrested LPS-induced inflammatory bone loss, decreased inflammatory infiltrate, and decreased osteoclastogenesis. This proof-of-concept study suggests a novel target using an intraoral RNA interference (RNAi) strategy to control periodontal inflammation.

INTRODUCTION

Periodontal diseases are chronic bacterial infections manifesting as soft tissue inflammation and alveolar bone loss, which eventually leads to tooth loss. Innate and acquired immune responses are both necessary to clear bacterial pathogens and to generate the inflammatory cascade that contributes to osteoclastogenic bone loss—a hallmark of periodontal disease. LPS from gram-negative periodontal pathogens are recognized by CD14, and Toll-like receptors, triggering intracellular signaling cascades, including the nuclear factor-kappa B (NF-κB) and MAPK pathways (Lee and Young, 1996; Rao, 2001). p38 MAPK, one of three distinct classes of MAP kinases, is a nexus for signal transduction, playing a vital role in numerous inflammatory-driven pathological processes including periodontitis. p38 MAPK signaling activation directly or indirectly mediates inflammatory cytokine expression such as interleukin (IL)-1β, IL-6, and tumor necrosis factor-alpha (TNF-α). These cytokines synergistically stimulate the production of other inflammatory cytokines, matrix metalloproteinases (MMPs), and prostanoids (Ridley et al., 1997; Ajizian et al., 1999; Dean et al., 1999; Underwood et al., 2000; Mbalaviele et al., 2006). Within the periodontal microenvironment, various cell types require p38 MAPK signaling as an integral component in the regulation of expression of pro-inflammatory cytokines and enzymes induced by inflammatory and infectious signals *in vitro*, including IL-6, MMP-13 and receptor activator of NF-κB ligand (RANKL) (Patil et al., 2004; Rossa et al., 2005; Patil et al., 2006; Rossa et al., 2007).

In vivo data suggest that p38 signaling is required for LPS-induced alveolar bone loss because small molecule p38 inhibitors were effective in reducing periodontitis in rodent models (Kirkwood et al., 2007; Rogers et al., 2007a). p38 MAPK inhibitors have been shown to be efficacious in other

small animal inflammatory disease models, but development of small molecule inhibitor therapeutics has been hampered by various unwanted side effects in clinical trials such as dermatoses and neurotoxicity.

MK2 is a direct substrate of p38 MAPK (Stokoe et al., 1992), and recent studies suggest a central role of MK2 in the production of pro-inflammatory mediators (Kotlyarov et al., 1999). One important mechanism by which MK2 increases expression of pro-inflammatory mediators is via targeting AU-rich elements located in the 3'-untranslated region of the mRNA via phosphorylation of RNA stability regulating proteins such as tristetraprolin (TTP) (Carballo et al., 1998; Chrestensen et al., 2004; Hitti et al., 2006). *In vivo* data suggest that overexpression of TTP decreased endogenous ARE cytokine levels and was protective against inflammation-induced bone loss via modulation of RNA stability (Patil et al., 2008). Although targeting MK2 with small molecular inhibitors is complex due to the relatively planar ATP binding site of this critical MAPK, targeting downstream signaling molecules such as MK2 represents a focused approach for regulating post-transcriptional expression of inflammatory mediators. Such an approach could reduce some of the deleterious effects of targeting key signaling intermediates such as p38 MAPK, thereby potentially decreasing side effects and increasing clinical efficacy.

RNAi can control gene expression, and microRNA and siRNA are central components of this technique, which has evolved from a target validation tool to a testing strategy for novel RNAi-based therapeutics. Still, at this time, no studies offer direct evidence that RNAi can be employed in the oral cavity, and no studies address the contribution of MK2 signaling in periodontal disease progression. RNAi silencing could provide an innovative anti-inflammatory

drug platform to selectively block signaling mechanisms needed for enhanced cytokine mRNA

stability/translation in periodontal disease progression. Our i*n vitro* and *in vivo* data suggest that

siRNA targeting of MK2 is a novel therapeutic platform for control of periodontal inflammation

and bone loss.

MATERIALS AND METHODS

Cell culture and Reagents

For *in vitro* studies, a rat macrophage cell line NR8383 was obtained from American Type Cell Collection (ATCC CRL-2192, Manassas, VA). Cells were grown in Ham's F12K medium (ATCC, Manassas, VA) supplemented with 15% heat inactivated fetal bovine serum (FBS, SAFC biosciences, Lenexa, KS), penicillin (50 IU/ml) and streptomycin (50 µg/ml; MP Biomedicals, Irvine, CA) in a 37 °C incubator with 5% CO_2. For *ex vivo* studies, rat bone marrow stromal cells were prepared by culturing bone marrow from the femurs/tibiae of donor rats (175–199 g) in alpha modified Eagle's medium (α-MEM, Invitrogen, Carlsbad, CA) containing 10% heat inactivated FBS, 10 ng/ml M-CSF (R&D Systems, Minneapolis, MN), 30% L929 conditioned medium, penicillin (50 IU/ml) and streptomycin (50 µg/ml) in a 37 °C incubator with 5% CO_2. The cells were cultured for 7 days before use. LPS was extracted from *A. actinomycetemcomitans* strain Y4 (serotype B) by the hot phenol-water method and purified, as previously described (Rogers et al., 2007b).

Small interfering RNA (siRNA) delivery

Accell MK2 siRNA (EQ-092297-00) and scrambled siRNA (D-001910-10) were purchased from Thermo Scientific/Dharmacon (Chicago, IL). For *in vitro* and *ex vivo* studies, cells were transfected siRNA utilizing the Accell siRNA delivery protocol and incubated for 72 h. For the *in vivo* study, covalently modified Accell siRNAs were locally injected.

Western blot

Cell lysates were prepared in ice-cold RIPA buffer (Cell Signaling Technology, Beverly, MA)

supplemented with proteinase inhibitor cocktails (Roche Diagnostics, Indianapolis, IN). After adjustment with NuPAGE® LDS Sample Buffer (Invitrogen, Carlsbad, CA), cell lysates were heated to 95 °C for 10 min. Equivalent amounts of proteins were separated by 10% Tris-HCl acrylamide gels and transferred to 0.2 µM nitrocellulose membranes (Bio-Rad Laboratories, Hercules, CA). Membranes were blocked with 5% w/v non-fat dry milk and 0.1% v/v Tween-20 in PBS, for 1–2 h at room temperature. The primary antibodies for total MK2, phospho-MK2 (Thr334), phospho-p38 MAPK (Thr180/Tyr182), phospho-SAPK/JNK (Thr183/Tyr185), phospho-p44/42 MAPK (Erk1/2, Thr202/Tyr204) and β-actin were purchased from Cell Signaling Technology (Beverly, MA). Primary antibodies were detected with HRP-conjugated secondary antibodies (Cell Signaling Technology, Beverly, MA) followed by chemiluminescent reaction with SuperSignal West Pico Chemiluminescent Substrate (Thermo Fisher Scientific, Rockford, IL). Radiographic images were obtained on a Gel-Doc XR system and densitometric analysis was performed using Quantity One Software (Bio-Rad, Hercules, CA).

ELISA

Cytokine expression in cell culture supernatant was measured using ELISA kits (R&D Systems, Minneapolis, MN) according to the manufacturer's instructions. The protein concentration in cell lysates was measured with a DC protein Assay Kit (Bio-Rad Laboratories, Hercules, CA). The concentration of cytokines was normalized by protein concentrations in cell lysates.

RNA isolation and qRT-PCR

Total RNA was isolated from treated and control cells at designated time points using TRIzol® (Invitrogen, Carlsbad, CA) according to the manufacturer's protocol and quantified on a

8

NanoDrop 1000 spectrophotometer (Thermo Fisher Scientific Inc). Using 300–500 ng total RNA in a 20 μl reaction, cDNA was prepared employing the High Capacity cDNA Reverse Transcription Kit (Applied Biosystems) in a C1000 Thermo Cycler (Bio-Rad) according to the manufacturer's suggested procedures. Quantitative real-time PCR was carried out using TaqMan Universal PCR Master Mix and TaqMan pre-designed primers (Applied Biosystems) on a StepOnePlus Real-Time PCR System (Applied Biosystems) under the following conditions: 50 °C for 2 min, 95 °C for 10 min, and 40 cycles of 95 °C for 15 sec, 60 °C for 1 min. The amplicon primers were obtained from Applied Biosystems for rat Mapkak2 (Rn01648144_g1), IL-6 (Rn01410330_m_1), TNF-α (Rn99999017_m_1), Ptgs2 (Rn01483828_m_1), IL-1β (Rn00580432_m_1), CXCL1 (Rn00578225_m_1) and β-actin (4352931E). Relative quantification was calculated by using the $\Delta\Delta$CT method and β-actin as the endogenous control was used to normalize target gene expression between wells. Expression levels were normalized to non-targeting control (β-actin) and reported as a percentage of the non-targeting control expression level.

Animals

The Institutional Animal Care and Use Committee (IACUC) at the Medical University of South Carolina approved all animal protocols. Adult male Sprague-Dawley rats (Harlan Laboratories, Inc., Indianapolis, IN) weighing ~250–274 g were used for *in vivo* study. Rats were maintained under specific pathogen-free conditions in pairs with food and tap water *ad libitum*. Once weekly, animals were routinely weighed to ensure proper growth and nutrition.

Experimental periodontitis model and administration of Accell siRNA in vivo

Inflammatory bone loss was initiated according to the aggressive periodontitis model described previously (Rogers et al., 2007b). The rats received one of the four following treatments: 2 µl of a 10 mg/ml solution of *A. actinomycetemcomitans* LPS three times per week plus mock injection PBS twice per week for 4 weeks ($n = 12$), LPS three times per week plus Accell MK2 siRNA or Accell Scrambled siRNA (4 nmol/injection) twice per week for 4 weeks ($n = 12$), and control groups given PBS vehicle five times per week for 4 weeks ($n = 12$). All direct injections were delivered to the palatal gingiva between the maxillary first and second molars via a 33-gauge Hamilton syringe. At the end of the experimental period, all animals were sacrificed by carbon dioxide asphyxiation. Maxillas were hemissected ($n = 12$/group) and posterior block sections were immersed directly in 10% buffered formalin fixative solution for 24 h and the transferred to 70% ethanol and kept at 4 °C.

Microcomputed Tomography (µCT)

As previously described, nondemineralized rat maxillae (n = 12/group) were scanned in 70% ethanol by a cone beam µCT system (GE Healthcare BioSciences, Chalfont St. Giles, UK) and the images were analyzed using GEHC MicroView software (version viz. + 2.0 build 0029). Briefly, each scan was reconstructed at a mesh size of $18 \times 18 \times 18$ µm to create a three-dimensional digitized image for each specimen. Then the images were rotated into a standard orientation and threshold at 1621 was used to distinguish between mineralized and nonmineralized tissue. The ROI for the Bone Volume Fraction (BVF) and Bone Mineral Density (BMD) analysis was based on several easily-identifiable anatomical landmarks. The BFV/BMDs were then calculated using the GE MicroView software's innate bone analysis module.

10

(Kirkwood et al., 2007; Patil et al., 2008; Sartori et al., 2009). All μCT scans were measured and assessed by an independent, masked examiner in a blinded manner.

Laser Capture Microdissection (LCM)

To measure expression of the siRNA target gene and inflammatory cytokine genes at the end of the experimental period in *in vivo* samples, quantitative real-time PCR was performed combined with LCM. Gingival tissue from sites of palatal injection were removed and immediately embedded in Tissue-Tek® OCT compound (Sakura Finetek USA, Torrance, CA), snap-frozen in liquid nitrogen and kept at -80 °C. Serial 8 μm thickness frozen sections were cut on a Digital Microtome Cryostat (Minotome *PLUS*™, Triangle Biomedical Science, Durham, NC) and mounted on superfrost/plus microscope slides. After the sections were stained with the HistoGene LCM Frozen Section Staining Kit (Molecular Devices, Sunnyvale, CA), LCM was employed using ArcturusXT™ Microdissection System (Arcturus; Molecular Devices, Sunnyvale, CA) to separate and collect connective tissue in which siRNA and LPS injections were performed. The tissue was transferred into a 0.5 ml tube and stored at -80 °C until utilized for RNA extraction. Total RNA was extracted and purified from the microdissected tissue with RNAqueous®-Micro Kit (Applied Biosystems, Foster City, CA) according to the manufacturer's instructions. The quantity and quality of RNA was assessed using an RNA 6000 Pico kit on an Agilent 2100 BioAnalyzer (Agilent Technologies, Santa Clara, CA). qRT-PCR was performed to measure target mRNA as described above.

Conventional histology and Tartrate Resistant Acid Phosphatase (TRAP) staining

Formalin-fixed, decalcified maxillae were paraffin embedded and serial sagittal sections (7

µm) prepared. Some slides were stained routinely with hematoxylin and eosin (H&E) for descriptive histology. Histological images were acquired using an Olympus BX61 Research (Center Valley, PA). Microscope outfitted with a DP71 digital camera. The degree of inflammation was quantified by counting the number of nuclei as a measure of cellular infiltrate using VIS image analysis module (Visopharm Inc., Hoersholm, Denmark). Pixel information that corresponded to "nuclei" was used to create a universal category that was then applied to all images, with the resulting objects that fit this classifier under a Bayesian analysis for counted nuclei. Approximately the same maxillary sections were used for histological analysis. Serial sections slides were submitted for TRAP staining method as described in the protocol from BD Biosciences (Technical Bulletin #445) to determine the number of osteoclasts. The multinucleated TRAP-positive cells that contained three or more nuclei and made contact with the bone surface were defined as osteoclasts. The number of osteoclasts within the eroded area was measured, and data were expressed as the total number of osteoclasts per section.

Statistical analysis

Between-group analyses were conducted using Student's t-test for 2 group comparison and analysis of variance (ANOVA) for multi-group comparison, applying GraphPad Prism (version 4; GraphPad Software, San Diego, CA). P values of 0.05 or less were considered significant.

JPET #172395

RESULTS

MK2 siRNA target validation is selective for MK2 after LPS challenge

To validate knockdown of MK2 by siRNA prior to *in vivo* use, target MK2 protein and mRNA were measured in rat macrophages. As seen in **Fig. 1a**, MK2 expression was significantly reduced after MK2 siRNA delivery. Densitometric analysis of data from four independent experiments revealed ~70% decrease in MK2 compared with scrambled siRNA control samples. Similarly, MK2 mRNA was reduced >90% in macrophages transfected with MK2 siRNA, compared with scrambled siRNA samples (**Fig. 1b**). A similar reduction was also observed in primary rat bone marrow stromal cells transfected with MK2 siRNA (data not shown).

To investigate the effects of MK2 knockdown on activated MAPKs, phosphorylated MAPKs were analyzed by immunoblot. As shown in **Fig. 1c**, total MK2 were reduced at all times in all experimental conditions in MK2 siRNA-treated cells compared with controls. Phospho-MK2 peaked at 60 min post-LPS treatment and then decreased at 120 min in either scrambled siRNA transfected or untreated cells. Importantly, after MK2 siRNA delivery phospho-MK2 expression was lower than in scrambled siRNA transfected or untreated cells. Phospho-p38 MAPK did significantly change under experimental conditions. Phospho-JNK (p54, p46) protein was significantly induced 30–120 min after LPS stimulation in MK2 siRNA-treated cells. Phospho-ERK (p44, p42) expression increased modestly at 30 min after LPS stimulation in all treated cells and peaked from 60–120 min.

MK2 siRNA arrested inflammatory mediator production and stimulated anti-inflammatory cytokine expression

13

MK2 plays a central role in cytokine production, and IL-6 and TNF-α are key cytokines in the pathogenesis of periodontitis. As depicted in **Figs. 2a**, **b**, compared with scrambled siRNA group, MK2 siRNA-treated cells had a 60.2% reduction in IL-6 protein and a 62.1% reduction for TNF-α protein 24–48 h after LPS stimulation. However, PGE$_2$ was undetectable (data not shown). Corresponding mRNA of IL-6, TNF-α, COX2, IL-1β, CXCL1 and IL-10 were quantified post-LPS stimulation for the indicated time periods in MK2 siRNA-treated cells. As shown in **Fig. 2c**, LPS-induced IL-6 expression in the MK2 siRNA-treated group decreased by 55.3% at 4 h and 22.0% at 8 h, compared with controls. Similarly, TNF-α mRNA expression (**Fig. 2d**) was reduced by 61.6% and 53.1% at 4 h and 8 h, respectively, compared with scrambled siRNA controls. Comparable data were obtained with other cytokines COX2 (**Fig. 2e**) and IL-1β (**Fig. 2f**), and the chemokine CXCL1 (**Fig. 2g**).

MK2 siRNA intraoral delivery silenced target MK2 gene expression and impeded alveolar bone loss in an A. actinomycetemcomitans LPS-induced periodontitis model

The significance of silencing MK2 was determined in an experimental model of periodontal disease. Initially, local MK2 mRNA knockdown in gingival tissues after MK2 siRNA intraoral delivery was measured. MK2 or scrambled siRNA was bilaterally microinjected in the palatal regions between the maxillary first molar and the second molar (n = 6 rats/group, 4 nmol/injection, two injections/week). On days 9 and 16 post siRNA delivery, rats were sacrificed and mRNA from gingival tissues in the immediate area was used to perform qRT-PCR for MK2 mRNA expression. As shown in **Fig. 3b**, MK2 was decreased 30.5% ± 14.97% and 50.76% ± 9.6% after the 3rd and 5th injections, respectively, compared with scrambled siRNA samples.

14

These differences were significant ($P < 0.05$) for both treatment groups, compared with the scrambled siRNA injection group.

Next, we investigated the ability of injected MK2 siRNA to prevent *A. actinomycetemcomitans* LPS-induced alveolar bone loss in an established 4-week model of rat periodontal bone loss (Rogers et al., 2007b) and siRNA delivery as described above. A schema of the experimental protocol is presented (**Fig. 3a**). μCT was used to evaluate the extent of alveolar bone destruction. Representative μCT isoform displays presented in **Fig. 3c** show a significant protective effect with MK2 siRNA-treated periodontal tissues compared with scrambled siRNA samples. Quantitative changes of bone loss measured from μCT data indicate that *A. actinomycetemcomitans* LPS-induced experimental periodontitis led to robust and significant bone loss ($P < 0.001$) between the vehicle group and the LPS-injected group (**Fig. 3d, 3e**). The μCT-determined BVF (**Fig. 3d**) of a standardized ROI (as highlighted) was reduced from 0.77 ± 0.03 in the vehicle group to 0.64 ± 0.07 in the LPS group. Injections of MK2 siRNA effectively attenuated LPS-induced alveolar bone loss as evidenced by a BVF of 0.69 ± 0.05, which is significantly larger than the BVF associated with scrambled siRNA injections ($P < 0.05$). BMD data (**Fig. 3e**) further corroborated BVF result in this *in vivo* study.

Inflammatory gene expression is attenuated by MK2 gene silencing in vivo

In vivo suppression of cytokine mRNA by MK2 siRNA in periodontal connective tissues was measured by qRT-PCR from tissues harvested by LCM (**Fig. 4a**). Connective tissues were used for these experiments because LPS and siRNA injections occurred in this region (**Figs. 4b-f**). We observed a trend towards reduced expression of MK2, TNF-α, IL-1β, COX2 and

15

CXCL1 mRNAs in gingival connective tissue samples from MK2 siRNA-injected sites in comparison with scrambled siRNA-injected sites. We did not detect IL-6 and IFN-γ mRNA expression in these samples.

MK2 siRNA in vivo delivery attenuated A. actinomycetemcomitans LPS-induced inflammatory infiltrate and osteoclastogenesis

Histological examination of periodontal tissues was used to evaluate the extent of inflammatory infiltrate (**Fig. 5a**). H&E staining indicated low levels of inflammatory cells in control samples. In contrast, a large amount of inflammatory cells, primarily neutrophils with scattered lymphocytes and macrophages, were associated with LPS injections with/without scrambled siRNA injections. Local delivery of MK2 siRNA clearly reduced the number of inflammatory cells, particularly neutrophils. A significant increase (p <0.01) in the number of cells was observed in LPS groups with/without scrambled siRNA treatment compared with the vehicle group. A significant reduction (p <0.05) in cell number occurred in the MK2 siRNA-injected group compared with LPS groups with/without scrambled siRNA treatment, indicating that MK2 siRNA delivery repressed the inflammatory response (**Fig. 5b**). TRAP staining for osteoclast formation (**Fig. 6a**) indicated that MK2 siRNA treatment significantly reduced osteoclasts (p<0.001), which were identified by morphological features (size and multinucleation) and compared with scrambled siRNA injection samples (**Fig. 6b**).

DISCUSSION

Our main findings are as follows: 1) silencing MK2 modulates the innate immune response triggered by bacterial LPS; 2) intraoral delivery of covalently-modified siRNA is effective for inhibiting target gene expression *in vivo*; and 3) siRNA-mediated inhibition of MK2 decreases periodontal disease severity *in vivo*. To our knowledge, ours is the first study to show that MK2 is critical in the pathogenesis of periodontitis and to evaluate the therapeutic potential of modulating MK2 activity in a periodontal disease model using a covalently-modified siRNA.

Local delivery of siRNA therapeutics is a promising platform for the treatment of orally related diseases, and until now, direct evaluation of intraoral siRNA delivery has not been reported in the literature. However, because oral mucosa is similar to vaginal mucosa, other studies may provide insight into oral disease mechanisms. For example, in a study with mouse vaginal mucosa, siRNA vaginal instillation silenced gene expression in the mouse vagina and ectocervix for at least nine days (Palliser et al., 2006). In our study, Accell siRNA was used to perform local delivery. This covalently-modified siRNA has been systemically delivered by intraperitoneal injection in an ovarian cancer model (Difeo et al., 2009). We observed that 9 or 16 days post-MK2 siRNA delivery, target gene expression was significantly decreased. However, further works should be done to elucidate the knock down effects on distant tissues from the injection site and more peripheral tissues. In related studies of locally delivered siRNA, target gene levels by siRNA intrathecal injection lasted ~5 days (Christoph et al., 2006). siRNA against apolipoprotein B was active in mice for only a few days, and after nine days, apolipoprotein B approached 70% of its initial level, whereas apolipoprotein B knockdown in non-human primates

17

was still effective after 11 days (Zimmermann et al., 2006).

In the periodontal microenvironment, microbial-associated molecular patterns derived from bacteria in the dental biofilm activate leukocytes, macrophages, osteoblasts, and fibroblasts to produce cytokines such as TNF-α, IL-6 and prostaglandin E$_2$. Thus, *in vivo*, various cell types participate in the pathogenesis of periodontal diseases. To study the potential role of siRNA therapeutics, total bone marrow cultures comprised of monocytes/macrophages, lymphocytes, and preosteoblasts/stromal cells—all part of the periodontal microenvironment—were used to evaluate the effect of MK2 knockdown by siRNA on LPS-induced cytokine expression. Our data show that LPS-induced IL-6 expression was significantly decreased, both at the mRNA and protein levels, a result consistent with previous observations in MK2$^{-/-}$ mice (Kotlyarov et al., 1999; Hegen et al., 2006). We also observed that MK2 siRNA delivery significantly reduced TNF-α mRNA and protein expression. Regulation of IL-6 and TNF-α expression via MK2 occurs at two different levels: IL-6 synthesis is regulated at the level of mRNA stability, and TNF-α is regulated mainly through an ARE-dependent translation efficiency mechanism (Neininger et al., 2002). However, other data also show that TTP is a direct substrate of MK2, controlling both the stability and translation of TNF-α mRNA (Carballo et al., 1998). The role of MK2 in the regulation of LPS-induced inflammatory cytokine gene expression is confirmed by significant reductions of mRNA expression for COX2, IL-1β, and chemokine CXCL1 in cells transfected with MK2 siRNA. In the present study, MK2 siRNA gene knockdown changed the activation of JNK and ERK MAPKs, suggesting the existence of crosstalk and compensatory mechanisms and underscoring the complexities of TLR signaling pathways.

In vivo evidence presented here suggests that silencing MK2 is a valid therapeutic target for the management of periodontal diseases. Local delivery of MK2 siRNA reduced alveolar bone loss in an LPS-induced periodontitis model. Multiple inflammatory signals can modulate the expression of receptor activator of NF-κB (Christoph et al., 2006), of its ligand (RANKL) and of osteoprotegerin, which comprise the cytokine network controlling osteoclastogenesis. It is well established that the production of proinflammatory cytokines correlate with inflammatory periodontal bone loss resulting from osteoclast differentiation and activation. MK2 siRNA attenuated the inflammatory infiltrate associated with *A. actinomycetemcomitans* LPS-induced bone loss in the present study. Concomitantly, MK2 siRNA resulted in a decrease in osteoclast formation, and a subsequent reduction in bone resorption. At the end of the experimental period, mRNA expression of MK2 and other inflammatory genes were examined in the gingival connective tissue by qRT-PCR. We observed a non-significant but distinct reduction on the expression of MK2 and of the inflammatory genes, findings that were consistent with *in vitro* results. Although MK2 silencing in this study resulted in a reduction of osteoclasts numbers and activity, we cannot rule out another plausible mechanism whereby MK2 silencing reduced the absolute numbers of osteoclast precursors recruited into the periodontal microenvironment. Ongoing experiments are addressing this possible mechanism.

In summary, our study using locally delivered siRNA for treatment of an oral-related disease provides strong evidence for proof-of principle. Our data show that MK2 has a fundamental role in the pathogenesis of periodontitis and that MK2 is a potential therapeutic target. Future studies with larger animal models or non-human primates with naturally occurring periodontitis can be

exploited to address the therapeutic effect of MK2 silencing and to develop a clinical approach

for intraoral delivery of siRNA.

ACKNOWLEDGEMENTS

AUTHORSHIP CONTRIBUTIONS

Participated in research design: Q. Li, C. Rossa, K. Kirkwood
Conducted experiments: Q. Li, C. Rossa, H. Yu, B. Herbert, A. Liu, K. Martin
Performed data analysis: Q. Li, R. Zinna, K. Kirkwood
Wrote or contributed to the writing of the manuscript: Q. Li, K. Kirkwood

JPET #172395

REFERENCES

Ajizian SJ, English BK and Meals EA (1999) Specific inhibitors of p38 and extracellular signal-regulated kinase mitogen-activated protein kinase pathways block inducible nitric oxide synthase and tumor necrosis factor accumulation in murine macrophages stimulated with lipopolysaccharide and interferon-gamma. *J Infect Dis* **179**:939-944.

Carballo E, Lai WS and Blackshear PJ (1998) Feedback inhibition of macrophage tumor necrosis factor-alpha production by tristetraprolin. *Science* **281**:1001-1005.

Chrestensen CA, Schroeder MJ, Shabanowitz J, Hunt DF, Pelo JW, Worthington MT and Sturgill TW (2004) MAPKAP kinase 2 phosphorylates tristetraprolin on in vivo sites including Ser178, a site required for 14-3-3 binding. *J Biol Chem* **279**:10176-10184.

Christoph T, Grunweller A, Mika J, Schafer MK, Wade EJ, Weihe E, Erdmann VA, Frank R, Gillen C and Kurreck J (2006) Silencing of vanilloid receptor TRPV1 by RNAi reduces neuropathic and visceral pain in vivo. *Biochem Biophys Res Commun* **350**:238-243.

Dean JL, Brook M, Clark AR and Saklatvala J (1999) p38 mitogen-activated protein kinase regulates cyclooxygenase-2 mRNA stability and transcription in lipopolysaccharide-treated human monocytes. *J Biol Chem* **274**:264-269.

Difeo A, Huang F, Sangodkar J, Terzo EA, Leake D, Narla G and Martignetti JA (2009) KLF6-SV1 is a novel antiapoptotic protein that targets the BH3-only protein NOXA for degradation and whose inhibition extends survival in an ovarian cancer model. *Cancer Res* **69**:4733-4741.

Hegen M, Gaestel M, Nickerson-Nutter CL, Lin LL and Telliez JB (2006) MAPKAP kinase

2-deficient mice are resistant to collagen-induced arthritis. *J Immunol* **177**:1913-1917.

Hitti E, Iakovleva T, Brook M, Deppenmeier S, Gruber AD, Radzioch D, Clark AR, Blackshear PJ, Kotlyarov A and Gaestel M (2006) Mitogen-activated protein kinase-activated protein kinase 2 regulates tumor necrosis factor mRNA stability and translation mainly by altering tristetraprolin expression, stability, and binding to adenine/uridine-rich element. *Mol Cell Biol* **26**:2399-2407.

Kirkwood KL, Li F, Rogers JE, Otremba J, Coatney DD, Kreider JM, D'Silva NJ, Chakravarty S, Dugar S, Higgins LS, Protter AA and Medicherla S (2007) A p38alpha selective mitogen-activated protein kinase inhibitor prevents periodontal bone loss. *J Pharmacol Exp Ther* **320**:56-63.

Kotlyarov A, Neininger A, Schubert C, Eckert R, Birchmeier C, Volk HD and Gaestel M (1999) MAPKAP kinase 2 is essential for LPS-induced TNF-alpha biosynthesis. *Nat Cell Biol* **1**:94-97.

Lee JC and Young PR (1996) Role of CSB/p38/RK stress response kinase in LPS and cytokine signaling mechanisms. *J Leukoc Biol* **59**:152-157.

Mbalaviele G, Anderson G, Jones A, De Ciechi P, Settle S, Mnich S, Thiede M, Abu-Amer Y, Portanova J and Monahan J (2006) Inhibition of p38 mitogen-activated protein kinase prevents inflammatory bone destruction. *J Pharmacol Exp Ther* **317**:1044-1053.

Neininger A, Kontoyiannis D, Kotlyarov A, Winzen R, Eckert R, Volk HD, Holtmann H, Kollias G and Gaestel M (2002) MK2 targets AU-rich elements and regulates biosynthesis of tumor necrosis factor and interleukin-6 independently at different post-transcriptional

23

levels. *J Biol Chem* **277**:3065-3068.

Palliser D, Chowdhury D, Wang QY, Lee SJ, Bronson RT, Knipe DM and Lieberman J (2006)

An siRNA-based microbicide protects mice from lethal herpes simplex virus 2 infection.

Nature **439**:89-94.

Patil C, Rossa C, Jr. and Kirkwood KL (2006) Actinobacillus actinomycetemcomitans

lipopolysaccharide induces interleukin-6 expression through multiple mitogen-activated

protein kinase pathways in periodontal ligament fibroblasts. *Oral Microbiol Immunol*

21:392-398.

Patil C, Zhu X, Rossa C, Jr., Kim YJ and Kirkwood KL (2004) p38 MAPK regulates IL-1beta

induced IL-6 expression through mRNA stability in osteoblasts. *Immunol Invest*

33:213-233.

Patil CS, Liu M, Zhao W, Coatney DD, Li F, VanTubergen EA, D'Silva NJ and Kirkwood KL

(2008) Targeting mRNA stability arrests inflammatory bone loss. *Mol Ther*

16:1657-1664.

Rao KM (2001) MAP kinase activation in macrophages. *J Leukoc Biol* **69**:3-10.

Ridley SH, Sarsfield SJ, Lee JC, Bigg HF, Cawston TE, Taylor DJ, DeWitt DL and Saklatvala J

(1997) Actions of IL-1 are selectively controlled by p38 mitogen-activated protein kinase:

regulation of prostaglandin H synthase-2, metalloproteinases, and IL-6 at different levels.

J Immunol **158**:3165-3173.

Rogers JE, Li F, Coatney DD, Otremba J, Kriegl JM, Protter TA, Higgins LS, Medicherla S and

Kirkwood KL (2007a) A p38 mitogen-activated protein kinase inhibitor arrests active

alveolar bone loss in a rat periodontitis model. *J Periodontol* **78**:1992-1998.

Rogers JE, Li F, Coatney DD, Rossa C, Bronson P, Krieder JM, Giannobile WV and Kirkwood KL (2007b) Actinobacillus actinomycetemcomitans lipopolysaccharide-mediated experimental bone loss model for aggressive periodontitis. *J Periodontol* **78**:550-558.

Rossa C, Jr., Liu M, Bronson P and Kirkwood KL (2007) Transcriptional activation of MMP-13 by periodontal pathogenic LPS requires p38 MAP kinase. *J Endotoxin Res* **13**:85-93.

Rossa C, Jr., Liu M, Patil C and Kirkwood KL (2005) MKK3/6-p38 MAPK negatively regulates murine MMP-13 gene expression induced by IL-1beta and TNF-alpha in immortalized periodontal ligament fibroblasts. *Matrix Biol* **24**:478-488.

Sartori R, Li F and Kirkwood KL (2009) MAP kinase phosphatase-1 protects against inflammatory bone loss. *J Dent Res* **88**:1125-1130.

Stokoe D, Campbell DG, Nakielny S, Hidaka H, Leevers SJ, Marshall C and Cohen P (1992) MAPKAP kinase-2; a novel protein kinase activated by mitogen-activated protein kinase. *EMBO J* **11**:3985-3994.

Underwood DC, Osborn RR, Bochnowicz S, Webb EF, Rieman DJ, Lee JC, Romanic AM, Adams JL, Hay DW and Griswold DE (2000) SB 239063, a p38 MAPK inhibitor, reduces neutrophilia, inflammatory cytokines, MMP-9, and fibrosis in lung. *Am J Physiol Lung Cell Mol Physiol* **279**:L895-902.

Zimmermann TS, Lee AC, Akinc A, Bramlage B, Bumcrot D, Fedoruk MN, Harborth J, Heyes JA, Jeffs LB, John M, Judge AD, Lam K, McClintock K, Nechev LV, Palmer LR, Racie T, Rohl I, Seiffert S, Shanmugam S, Sood V, Soutschek J, Toudjarska I, Wheat AJ, Yaworski

E, Zedalis W, Koteliansky V, Manoharan M, Vornlocher HP and MacLachlan I (2006)

RNAi-mediated gene silencing in non-human primates. *Nature* **441**:111-114.

JPET #172395

FOOTNOTES

FIGURE LEGENDS

Figure 1. (a) MK2 protein expression was inhibited by specific MK2 siRNA in rat macrophage NR8383. (b) In rat macrophage NR8383, left panel: Densitometer scans of MK2 and β-actin were performed and recorded as the ratio of MK2 to β-actin. Density analysis showed significant knockdown of MK2 protein by MK2 siRNA delivery. right panel: qRT-PCR data validated the knockdown effect on MK2 mRNA expression after specific MK2 siRNA delivery. **P <0.01 and ***P <0.001. (c) A total of 3×10^5 rat macrophages NR8383 were grown in each well of six-well plate and either transfected with MK2 siRNA or scrambled siRNA for 72 h. Then the cells were either unstimulated (0 min) or stimulated with 1 µg/ml of LPS for various time periods (10, 30, 60, and 120 min). The MK2, phospho-MK2, phospho-p38, phospho-JNK (p54, p46) and phospho-ERK (p44, p42) were examined. β-actin used for loading control. Data are representative of three separate experiments.

Figure 2. MK2 siRNA delivery potently decreased expression of inflammatory mediates in rat bone marrow stromal cells. Rat BMSCs plated at 1.25×10^5 cells/well in 24-well plate were transfected with either Accell MK2 siRNA or scrambled siRNA for 72 hours. Cells were then stimulated with *A. actinomycetemcomitans* LPS (100 ng/ml) for an additional 24 or 48 h, respectively. Cell culture supernatants were harvested and IL-6 (a) and TNF-α (b) was measured with ELISA. Or cells were stimulated with *A. actinomycetemcomitans* LPS (100 ng/ml) for the indicated times and RNA was isolated for qRT-PCR to assay IL-6 (c), TNF-α (d), COX2 (e), IL-1β (f) and CXCL1 (g) mRNA levels. Results are expressed as mean ± SD of triplicate or quadruplicate samples. The data are representative of four independent experiments. *P <0.05,

**P* <0.01, and ****P* <0.001.

Figure 3. Specific MK2 siRNA *in vivo* delivery silenced target gene expression and reduced LPS-induced bone loss. (a) A schematic showing overall experimental protocol. (b) MK2 mRNA expression in palate gingiva after 3 and 5 times siRNA *in vivo* delivery. Results are expressed as mean ± SE (n = 5 or 6 rats/group, *P* < 0.05). (c) Representative μCT images of rat maxillae from indicated treatment groups. ROI for quantitative analysis is highlighted. (d) Volumetric analysis of bone loss levels. (e) Bone mineral density (BMD) analysis of bone loss levels. (**P* <0.05, ****P* <0.001).
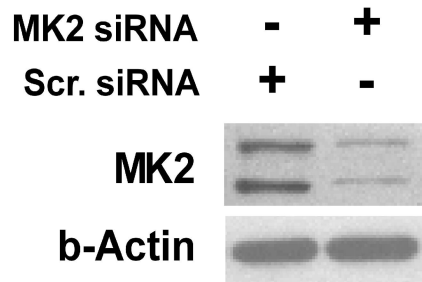
Figure 4. LCM was used to isolate mRNA for inflammatory gene expression levels in gingival connective tissue. (a) LCM procedure shows before and after connective tissue was captured from the section of rat palatal gingiva. Connective tissue, devoid of epithelium, was shown on the adhesive cap. (b-f) qRT-PCR results for identified genes in isolated connective tissue collected by LCM. Relative expression was determined from analysis of duplicate samples and calculated with respect to vehicle PBS control. The dotted line denotes the basement membrane that separates the connective tissue from the epithelium.

Figure 5. (a) MK2 silencing reduced inflammatory infiltrate induced by *A. actinomycetemcomitans* LPS in the area adjacent to bone loss. The representative sections on the left panel showed histological features from indicated treatment group (bars = 1,500 μm). The right panel showed enlarged box area at high magnification from the left panel with detailed information (bars = 60 μm). (b) Enumerated nuclei in each treatment group are presented. Results are expressed as mean ± SE (n = 5 or 6 rats/group, *P* <0.05, **P* <0.01).
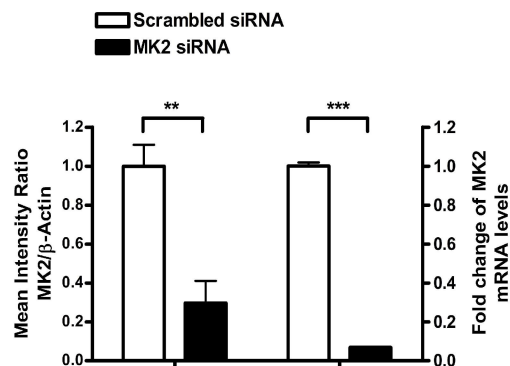
29

Figure 6. MK2 siRNA delivery attenuated osteoclastogenesis induced by *A. actinomycetemcomitans* LPS. (a) TRAP staining of representative tissue sections of rat maxillae from indicated treatment groups (bars = 100 μm). TRAP$^+$ osteoclasts were stained red. B = Bone, T = Tooth, dotted line shows area of bone, arrow indicates osteoclast. (b) Graphic representation of enumerated TRAP$^+$ multinucleated formation in each tissue section is presented. Horizontal bar indicates mean TRAP$^+$ cell counts. ** P <0.01, *** P <0.001.
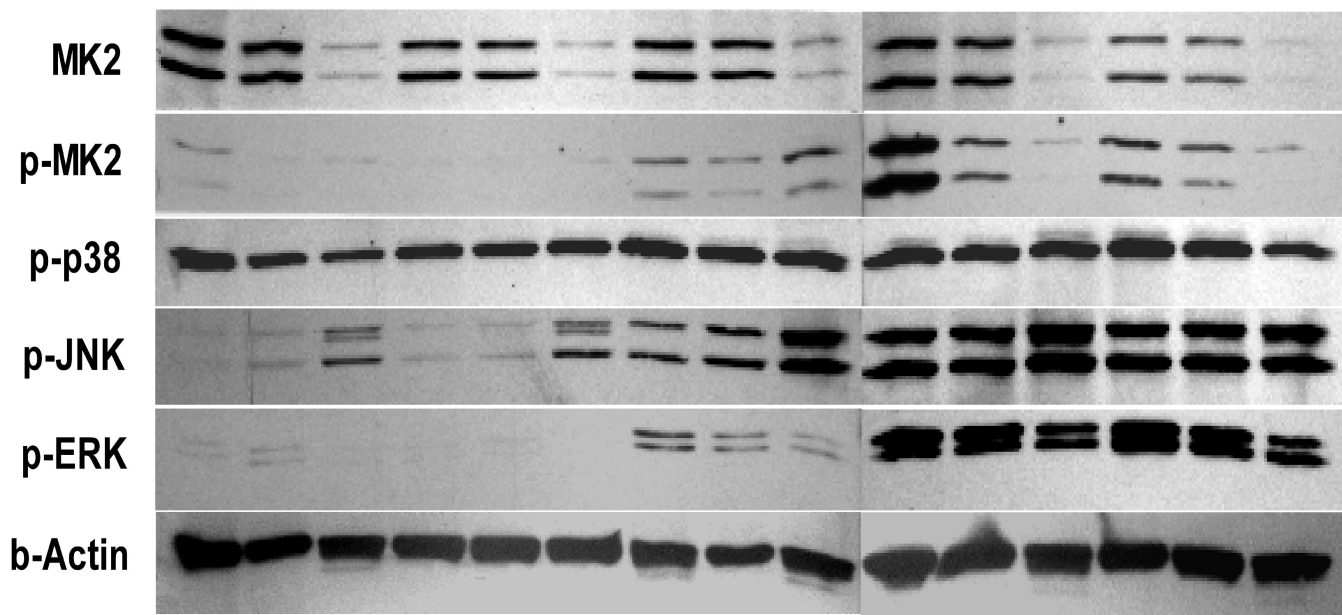
Fig. 1 JPET #172395

a

MK2 siRNA   −   +
Scr. siRNA   +   −

MK2

b-Actin

b

Scrambled siRNA
MK2 siRNA

Mean Intensity Ratio MK2/β-Actin

Fold change of MK2 mRNA levels

**

***

c

LPS   0   10   30   60   120   Min
MK2 siRNA   − − +   − − +   − − +   − − +   − − +
Scr. siRNA   − + −   − + −   − + −   − + −   − + −
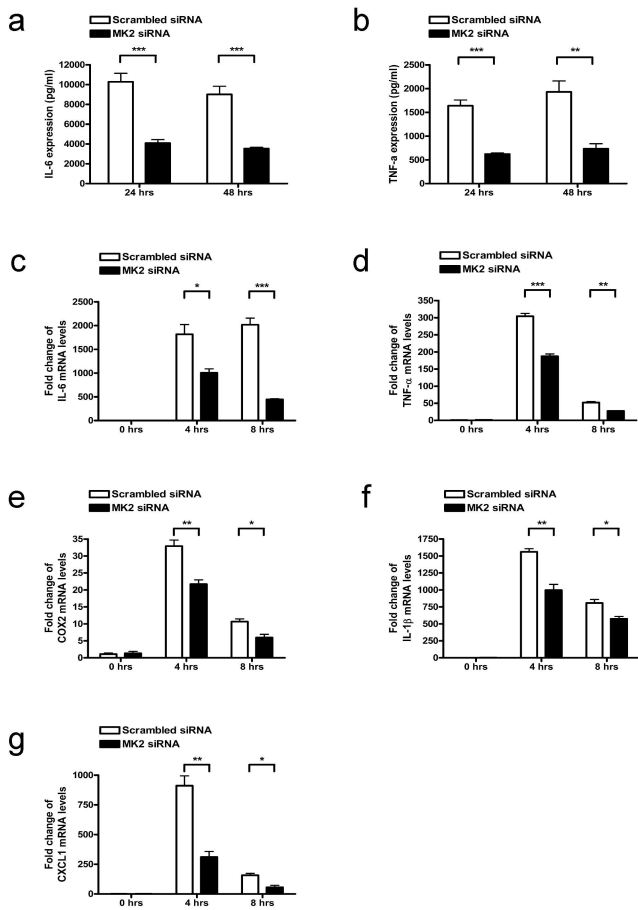
MK2

p-MK2

p-p38

p-JNK

p-ERK

b-Actin

Fig. 2 JPET #172395

Fig. 3 JPET #172395

Fig. 4 JPET #172395

Fig. 5 JPET #172395

a

b

Fig. 6 JPET #172395